primary imidazole–PF_6^- interactions are through the methyl groups off N(9) and (7). There is also some evidence (Table VIII) that the terminal amino groups of the dien chelate form weak hydrogen bonds with two of the fluorine atoms of the P(1)-containing PF_6^- anion.

There seems to be no evidence of base–base stacking interactions in this largely ionic structure.

B. [(dien)Pt(7,9-Dmhyp)]$(PF_6)_2 \cdot 1.5H_2O$. For this structure, three features dominate the crystal packing: Coulombic interactions between the ionic components, intermolecular hydrogen bonding, and a complex set of hydrogen bonds involving the waters of crystallization (Figures 7 and 8 and Table VIII). In describing this rather complex structure, we have divided the sets of interactions into two classes—those within the (010) crystallographic plane (Figure 7) and those which give rise to a columnar array along the [010] direction.

Within the (010) crystallographic plane, the complex cations are associated into dimeric pairs about the twofold axes along *b* (Figure 7). One of the specially positioned PF_6^- anions [P(1)] lies on the twofold axis along *b* and acts as a pivot for the coupling of two symmetry-related complex cations. Direct hydrogen bonding between the centrally located PF_6^- anion and one of the terminal amino groups of the dien chelate is observed, as well as a water bridge system utilizing the general position water molecule, W(1), and N(3) of the 7,9-Dmhyp base and the PF_6^- anion (Figure 7). Interactions between these dimeric units are mainly electrostatic in nature, with the methyl substituents off the imidazole ring of the purine ligand primarily involved.

Joining these highly interactive planes are columnar arrays (Figure 8) paralleling the crystallographic *b* axis. The sequence of components along this columnar array is as follows: (a) the specially positioned PF_6^- anion containing P(1) associated with two complex cations and water, W(1), molecules through hydrogen bonds, (b) the specially positioned PF_6^- anion containing P(2) which is electrostatically coupled to the methyl substituents of the purine bases associated with the P(1) PF_6^- anion, and finally, (c) the water molecule W(2) which is positioned on the twofold axis and hydrogen bonded to two general position PF_6^- anions, P(3).

Again, as in the 7,9-Dmgua structure, there is no evidence of base–base stacking interactions in the 7,9-Dmhyp crystal structure.

Summary

We find that the complex cations $[(dien)Pt(7,9\text{-}Dmgua)]^{2+}$ and $[(dien)Pt(7,9\text{-}Dmhyp)]^{2+}$ provide the first examples of type I Pt(II)–N(1)-bound 6-oxopurine complexes. Intramolecular interligand hydrogen bonding and Pt···O(6) interactions are integral features of both complexes. Intracomplex hydrogen bonding is the more important of the two interactions in the 7,9-Dmhyp complex, while the Pt···O(6) distance is shorter in the 7,9-Dmgua complex. The Pt···O(6) interaction in the 7,9-Dmgua complex is similar in apparent strength to that found in several Pt(II)–cytosine systems but substantially stronger than observed in type I Pt(II)–N(7)-bound 6-oxopurine complexes. The difference in the mode of interaction of the (dien)Pt moiety and the 7,9-Dmgua and 7,9-Dmhyp bases is proposed to arise largely as a consequence of the changes in molecular geometry needed to relieve the steric strain between the 2-amino substituent of the 7,9-Dmgua ring and the (dien)Pt group. In addition to its role in the interligand hydrogen bonding and the Pt(II) binding, O(6) of each base participates in intercomplex hydrogen bonding in the crystalline state. Otherwise, the crystal structures encompass general coulombic forces as well as complex hydrogen bonding arrays to achieve stability.

Acknowledgment. This investigation was supported by the National Institutes of Health, Public Health Service Grants GM 20544 and GM 29222. We thank Matthey Bishop, Inc., for a loan of K_2PtCl_4.

Registry No. $[(dien)(7,9\text{-}Dmgua)Pt^{II}](PF_6)_2$, 76900-59-9; $[(dien)(7,9\text{-}Dmhyp)Pt^{II}](PF_6)_2 \cdot 1.5H_2O$, 76915-23-6; $Pt(dien)I_2$, 18509-61-0.

Supplementary Material Available: Tables of nonhydrogen atom anisotropic thermal parameters and parameters for the hydrogen atoms and a list of calculated and observed structure factor amplitudes (77 pages). Ordering information is given on any current masthead.

Contribution from the Department of Chemistry,
Massachusetts Institute of Technology, Cambridge, Massachusetts 02139

Preparation and Reactions of $[ZrCl_3(PR_3)_2]_2$ (R = Et, Pr, Bu) and X-ray Structure of $[ZrCl_3(PBu_3)_2]_2$

JEFFREY H. WENGROVIUS, RICHARD R. SCHROCK,*[1] and CYNTHIA S. DAY

Received October 30, 1980

Complexes of the type $[ZrCl_3(PR_3)_2]_2$ (R = Et, Pr, Bu) have been prepared in high yield by reducing $ZrCl_4(PR_3)_2$ with 1 equiv of sodium amalgam. The X-ray structure of $[ZrCl_3(PBu_3)_2]_2$ shows it to be a chloride-bridged dimer with a Zr–Zr bond distance of 3.182 (1) Å. $[ZrCl_3(PBu_3)_2]_2$ crystallizes in the monoclinic space group $C2/c$ with $a = 26.570$ (6) Å, $b = 15.287$ (3) Å, $c = 16.452$ (3) Å, and $\beta = 97.18$ (2)°. The structure was solved by standard Patterson and difference-Fourier methods to values of $R_1 = 5.3\%$ and $R_2 = 6.2\%$ for 4720 reflections having $2\theta_{\mathrm{Mo}\,K\alpha} < 55°$ and $I > 3\sigma(I)$. The molecule has a distorted octahedral geometry about each Zr and cis phosphine ligands in the same plane as the bridging chloride ligands. $[ZrCl_3(PR_3)_2]_2$ reacts with ethylene and propylene to give Zr(IV) complexes, $(PR_3)_2Cl_3ZrCH_2CHRZrCl_3(PR_3)_2$ (R = H or Me). On reaction with butadiene, $[ZrCl_3(PEt_3)_2]_2$ disproportionates to $ZrCl_4(PEt_3)_2$ and $ZrCl_2(\eta^6\text{-}C_8H_{12})(PEt_3)$; $\eta^6\text{-}C_8H_{12}$ is the well-known bis allyl ligand formed by coupling two butadiene molecules.

Introduction

We recently reported[2] our unsuccessful attempts to prepared a zirconium–neopentylidene complex by promoting loss of neopentane from $Zr(CH_2CMe_3)_2Cl_2(PMe_3)_2$ thermally or photochemically. Photolysis gave a sparingly soluble, forest green crystalline product with the composition $ZrCl_3(PMe_3)_2$ in ca. 60% yield vs. Zr. Since this compound was diamagnetic and showed only PMe_3 ligands by ^1H NMR, we proposed it was dimeric with a Zr–Zr bond and two bridging chloride ligands. This would be the first example of a complex containing a Zr–Zr bond and the only member so far of the class of adducts of $\beta\text{-}ZrCl_3$ which is nicely soluble and easy to

---

[1] To whom correspondence should be addressed.

[2] Wengrovius, J. H.; Schrock, R. R. *J. Organomet. Chem.* **1981**, *205*, 319–322.

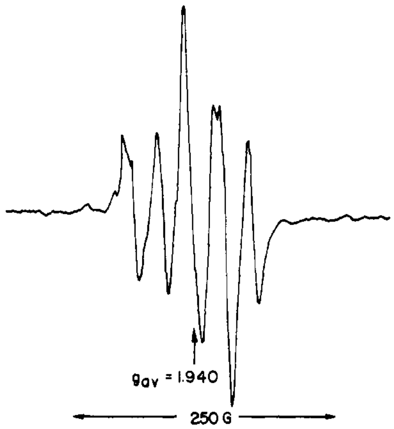

Figure 1. ESR spectrum of $[ZrCl_3(PEt_3)_2]_2 + \sim 10PEt_3$ in toluene (T = 25 °C).

characterize. Therefore, we set out to prepare this product directly by reducing Zr(IV) and, in particular, to prepare more soluble compounds by using longer chain alkylphosphines.

Results

Preparation and Characterization. $[ZrCl_3L_2]_2$ complexes can be prepared by reducing $ZrCl_4L_2$ with sodium amalgam in toluene under nitrogen or argon (eq 1). As we expected,

$$ZrCl_4 + 2L \xrightarrow[Na/Hg]{toluene} 0.5[ZrCl_3L_2]_2 \qquad (1)$$

$$L = PMe_3, PEt_3, PPr_3, PBu_3$$

we could not separate the sparingly soluble PMe_3 complex from the finely divided mercury and sodium chloride remaining after reduction. However, the PEt_3, PPr_3, and PBu_3 products are increasingly soluble in benzene and toluene and therefore could be characterized fully.

The molecular weights (cryoscopic) for these compounds are between those expected for monomers and those expected for dimers, and they are concentration dependent. However, in the presence of 1 equiv of PEt_3, the molecular weight for $[ZrCl_3(PEt_3)_2]_2$ (corrected for the added PEt_3) is close (812) to the expected value (868). These results suggest that PEt_3 is reversibly lost in solution (eq 2).

$$Zr_2Cl_6L_4 \rightleftharpoons L + Zr_2Cl_6L_3 \qquad (2)$$

^1H and ^{31}P NMR spectra confirm that free and coordinated phosphine exchange at a rate on the order of the NMR time scale. The ^1H NMR spectra show only one set of phosphine resonances, even when free phosphine is added. The ^{31}P NMR spectra show a broad peak for bound phosphine which sharpens but does not shift significantly, when the temperature is lowered; only a small peak for free phosphine is observed in the low-temperature spectrum. When free phosphine is added, the room-temperature ^{31}P NMR spectrum shows a broad resonance for coordinated phosphine and a broad resonance for free phosphine. When this sample is cooled (−40 °C), only the peak for *coordinated* phosphine sharpens. No other peaks are observed. We propose that (i) there are two ways to exchange phosphines, the one shown in eq 2 and a second shown in eq 3, and (ii) the peak for free phosphine in the −40 °C spectrum is broadened by exchange with phosphine in a Zr(III) complex.

$$0.5Zr_2Cl_6L_4 \rightleftharpoons ZrCl_3L_2 \underset{-L}{\overset{+L}{\rightleftharpoons}} ZrCl_3L_3 \qquad (3)$$

A weak ESR signal (Figure 1) for solutions of $[ZrCl_3L_2]_2$ and L is good evidence that a Zr(III) species is present. The six-line hyperfine pattern typical of Zr(III)[3] (^{91}Zr has a $S = {}^5/_2$, (11.2% natural abundance)) could not be observed at the resolution of our instrument. Since the signal qualitatively becomes more intense when excess L is added, we believe the Zr(III) species is most likely $ZrCl_3L_3$. Determination of susceptibilities of $[ZrCl_3L_2]_2$ samples by Evans' method was not accurate enough to say unambiguously that the susceptibility increased in the presence of excess phosphine, although qualitatively the results were consistent with this hypothesis.

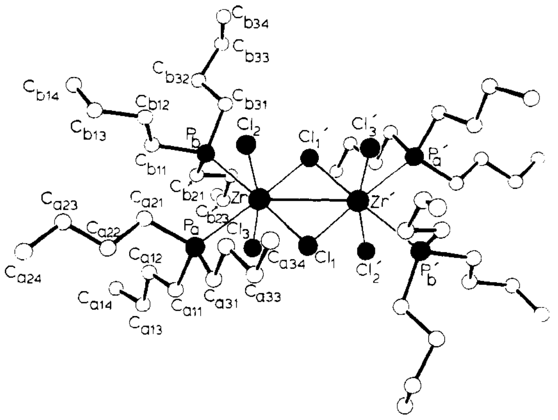

Figure 2. Molecular structure of $[ZrCl_3(PBu_3)_2]_2$ (drawing adapted from an ORTEP plot using arbitrarily sized spheres).

Table I[a]

atom type[b]	fractional coordinates		
	x	y	z
Zr	0.208 89 (2)	0.198 25 (3)	0.439 70 (3)
Cl_1	0.303 21 (5)	0.166 65 (10)	0.474 77 (9)
Cl_2	0.180 24 (6)	0.096 81 (10)	0.538 24 (8)
Cl_3	0.219 87 (6)	0.282 02 (10)	0.317 72 (9)
P_a	0.216 21 (6)	0.048 94 (10)	0.339 27 (8)
P_b	0.103 73 (6)	0.226 03 (12)	0.395 60 (10)
C_{a11}	0.221 39 (23)	0.074 43 (44)	0.231 06 (33)
C_{a12}	0.169 61 (25)	0.105 91 (47)	0.185 95 (37)
C_{a13}	0.177 47 (35)	0.145 86 (55)	0.102 43 (44)
C_{a14}	0.125 09 (43)	0.168 86 (75)	0.055 30 (56)
C_{a21}	0.165 58 (23)	−0.034 48 (38)	0.335 52 (35)
C_{a22}	0.173 87 (26)	−0.116 30 (43)	0.284 12 (39)
C_{a23}	0.12758 (30)	−0.177 28 (49)	0.277 67 (46)
C_{a24}	0.136 57 (38)	−0.259 60 (58)	0.228 68 (56)
C_{a31}	0.275 94 (23)	−0.013 63 (42)	0.365 15 (36)
C_{a32}	0.275 96 (28)	−0.058 40 (48)	0.451 48 (43)
C_{a33}	0.330 71 (36)	−0.091 08 (63)	0.480 70 (55)
C_{a34}	0.331 77 (44)	−0.133 41 (89)	0.565 61 (61)
C_{b11}	0.062 34 (26)	0.133 82 (57)	0.355 95 (48)
C_{b12}	0.057 19 (30)	0.063 08 (57)	0.419 22 (51)
C_{b13}	0.023 69 (35)	−0.020 74 (79)	0.384 29 (68)
C_{b14}	−0.029 04 (43)	0.000 67 (102)	0.370 34 (72)
C_{b21}	0.087 61 (33)	0.302 61 (72)	0.308 65 (58)
C_{b22}	0.102 90 (43)	0.395 87 (74)	0.326 79 (85)
C_{b23}	0.099 66 (98)	0.448 76 (153)	0.241 01 (156)
C_{b24}	0.074 62 (138)	0.497 55 (182)	0.226 84 (200)
C_{b31}	0.072 74 (25)	0.270 01 (51)	0.481 13 (46)
C_{b32}	0.014 66 (31)	0.288 36 (73)	0.459 87 (66)
C_{b33}	−0.005 04 (59)	0.345 22 (151)	0.531 09 (119)
C_{b34}	−0.007 25 (82)	0.293 58 (165)	0.594 45 (127)

[a] The numbers in parentheses are the estimated standard deviations in the last significant digit. [b] Atoms are labeled in agreement with Figure 2.

Structure of $[ZrCl_3(PBu_3)_2]_2$. A drawing of the structure is shown in Figure 2. Final atomic coordinates for all atoms can be found in Table I and anisotropic thermal parameters for the nonhydrogen atoms in Table II.[4] Bond lengths and

---

(3) Lappert, M. F.; Riley, P. I.; Yarrow, P. I. W. *J. Chem. Soc., Chem. Commun.* **1979**, 305–306.

(4) See paragraph at end of paper regarding supplementary material.

Table III

Bond Lengths Involving Nonhydrogen Atoms[a]

type[b]	length, Å	type[b]	length, Å
$P_a{-}C_{a11}$	1.844 (6)	$P_b{-}C_{b11}$	1.855 (8)
$P_a{-}C_{a21}$	1.849 (6)	$P_b{-}C_{b21}$	1.857 (10)
$P_a{-}C_{a31}$	1.856 (6)	$P_b{-}C_{b31}$	1.844 (8)
$C_{a11}{-}C_{a12}$	1.556 (9)	$C_{b11}{-}C_{b12}$	1.519 (12)
$C_{a12}{-}C_{a13}$	1.542 (10)	$C_{b12}{-}C_{b13}$	1.624 (14)
$C_{a13}{-}C_{a14}$	1.547 (14)	$C_{b13}{-}C_{b14}$	1.429 (15)
$C_{a21}{-}C_{a22}$	1.541 (9)	$C_{b21}{-}C_{b22}$	1.502 (16)
$C_{a22}{-}C_{a23}$	1.536 (10)	$C_{b22}{-}C_{b23}$	1.619 (28)
$C_{a23}{-}C_{a24}$	1.529 (12)	$C_{b23}{-}C_{b24}$	1.007 (40)
$C_{a31}{-}C_{a32}$	1.577 (9)	$C_{b31}{-}C_{b32}$	1.564 (11)
$C_{a32}{-}C_{a33}$	1.556 (12)	$C_{b32}{-}C_{b33}$	1.599 (23)
$C_{a33}{-}C_{a34}$	1.537 (14)	$C_{b33}{-}C_{b34}$	1.315 (31)

Bond Angles Involving Nonhydrogen Atoms[a]

type[b]	angle, deg	type[b]	angle, deg
$ZrCl_1Zr'$	77.43 (4)		
ZrP_aC_{a11}	114.2 (2)	ZrP_bC_{b11}	119.9 (3)
ZrP_aC_{a21}	118.1 (2)	ZrP_bC_{b21}	114.7 (3)
ZrP_aC_{a31}	113.6 (2)	ZrP_bC_{b31}	112.3 (2)
$C_{a11}P_aC_{a21}$	104.8 (3)	$C_{b11}P_bC_{b21}$	98.0 (4)
$C_{a11}P_aC_{a31}$	99.5 (3)	$C_{b11}P_bC_{b31}$	104.1 (3)
$C_{a21}P_aC_{a31}$	104.5 (3)	$C_{b21}P_bC_{b31}$	106.0 (4)
$P_aC_{a11}C_{a12}$	111.0 (4)	$P_bC_{b11}C_{b12}$	113.6 (6)
$P_aC_{a21}C_{a22}$	115.1 (4)	$P_bC_{b21}C_{b22}$	114.5 (7)
$P_aC_{a31}C_{a32}$	109.5 (4)	$P_bC_{b31}C_{b32}$	114.6 (6)
$C_{a11}C_{a12}C_{a13}$	109.7 (6)	$C_{b11}C_{b12}C_{b13}$	114.3 (7)
$C_{a12}C_{a13}C_{a14}$	108.9 (7)	$C_{b12}C_{b13}C_{b14}$	111.0 (9)
$C_{a21}C_{a22}C_{a23}$	111.2 (6)	$C_{b21}C_{b22}C_{b23}$	108.5 (12)
$C_{a22}C_{a23}C_{a24}$	111.1 (6)	$C_{b22}C_{b23}C_{b24}$	122.2 (28)
$C_{a31}C_{a32}C_{a33}$	108.2 (6)	$C_{b31}C_{b32}C_{b33}$	109.7 (10)
$C_{a32}C_{a33}C_{a34}$	109.0 (7)	$C_{b32}C_{b33}C_{b34}$	107.8 (16)

Polyhedral Edge Lengths and Bond Lengths Subtended at the Zr Atom[a]

type[b]	length, Å	type[b]	length, Å
$Zr\cdots Zr'$ [c]	3.182 (1)	$Cl_1\cdots Cl_1'$ [c]	3.970 (2)
		$Cl_1\cdots Cl_2$	3.709 (2)
$Zr{-}Cl_1$	2.546 (1)	$Cl_1\cdots Cl_3$	3.641 (2)
$Zr{-}Cl_1'$ [c]	2.542 (2)	$Cl_1\cdots P_a$	3.502 (2)
		$Cl_1\cdots P_b$	3.469 (2)
$Zr{-}Cl_2$	2.433 (2)	$Cl_1'\cdots Cl_2$ [c]	3.652 (2)
$Zr{-}Cl_3$	2.429 (2)	$Cl_1'\cdots Cl_3$ [c]	3.629 (2)
		$Cl_2\cdots P_a$	3.598 (2)
$Zr{-}P_a$	2.839 (2)	$Cl_2\cdots P_b$	3.514 (2)
$Zr{-}P_b$	2.830 (2)	$Cl_3\cdots P_a$	3.583 (2)
		$Cl_3\cdots P_b$	3.590 (2)
$P_a\cdots P_b$	4.221 (2)	$Cl_2\cdots Cl_3'$ [c]	3.810 (2)

Polyhedral Bond Angles Subtended at the Zr Atom[a]

type[b]	angle, deg	type[b]	angle, deg
P_aZrP_b	96.25 (5)	$Cl_1'ZrCl_2$ [c]	94.43 (5)
Cl_1ZrCl_1' [c]	102.57 (5)	$Cl_1'ZrCl_3$ [c]	93.75 (5)
Cl_1ZrCl_2	96.27 (5)	$Cl_1'ZrP_a$ [c]	176.45 (5)
Cl_1ZrCl_3	94.06 (5)	$Cl_1'ZrP_b$ [c]	80.26 (5)
Cl_1ZrP_a	80.93 (5)	Cl_2ZrP_a	85.72 (5)
Cl_1ZrP_b	177.17 (5)	Cl_2ZrP_b	83.41 (5)
Cl_2ZrCl_3	165.11 (6)	Cl_3ZrP_a	85.35 (5)
		Cl_3ZrP_b	85.74 (5)

[a] The numbers in parentheses are the estimated standard deviations in the last significant digit. [b] Atoms are labeled in agreement with Figure 2. [c] Atoms Cl_1', P_b', and Cl_3' are related to atoms Cl_1, P_b, and Cl_3, respectively, by the symmetry operation $^1/_2 - x, {}^1/_2 - y, 1 - z$ where the atomic coordinates (x, y, z) for Cl_1, P_b, and Cl_3 are given in the accompanying table.

bond angles can be found in Table III.

The molecule is a dimer with a distorted octahedral geometry about each Zr but a nearly planar eight-atom unit consisting of the two metals, the two bridging chlorides, and the four phosphorus nuclei. (The maximum displacement of any atom in the group from the least-squares mean plane is 0.01 Å.) There are three main distortions from octahedral geometry. The first is a bending back of each of the four terminal chloride ligands away from the central four-atom 2Zr2Cl unit by 7–8°; for example, the Cl_2–Zr–Cl_3 bond angle is 165.11 (6)° (see Table III). This distortion can be ascribed largely to steric repulsions between the axial chloride ligands on adjacent metals since without it the $Cl_2\cdots Cl_3'$ contact (3.810 Å) would be an unacceptably short 3.18 Å, the $Zr\cdots Zr'$ distance (see below). The second distortion is a larger than expected P_a–Zr–P_b angle (96.25 (5)°) which can be ascribed to repulsion between the two bulky phosphine ligands. The third distortion, a large Cl_1–Zr–Cl_1' angle (102.57 (5)°), can be ascribed to formation of a Zr–Zr single bond (3.182 (1) Å). The Zr–Cl_1–Zr angle therefore is substantially less than 90° (77.43 (4)°), and the $Cl_1\cdots Cl_1'$ distance (3.970 (2) Å) is 0.37 Å larger than the van der Waals diameter for Cl.[5]

Although the structural parameters for phosphine ligand a are unexceptional, those for phosphine ligand b are abnormal. The abnormal lengths of some bonds is phosphine ligand b presumably result from disorder in the respective alkyl chains. All attempts to improve these parameters during structural refinement were unsuccessful.

Some Reactions of $[ZrCl_3L_2]_2$. We looked at some simple reactions of $[ZrCl_3L_2]_2$ in order to determine whether the Zr–Zr bond, as we suspected, could be broken easily.

The first indication that $[ZrCl_3L_2]_2$ was a good reducing agent was its reaction with TlC_5H_5 to give thallium metal quantitatively and $ZrCpCl_3(PEt_3)_2$ (eq 4). $ZrCpCl_3(PEt_3)_2$

$$[ZrCl_3(PEt_3)_2]_2 + 2TlCp \xrightarrow{\text{toluene}} 2Tl + 2ZrCpCl_3(PEt_3)_2 \qquad (4)$$

was characterized by ^1H NMR comparison with an independently prepared sample.

$[ZrCl_3(PEt_3)_2]_2$ and $[ZrCl_3(PBu_3)_2]_2$ react with 1 equiv or an excess of ethylene to give orange, crystalline complexes. The PEt_3 complex could not be characterized well due to its low solubility in toluene. However, the PBu_3 complex is pentane soluble. It has a molecular weight (cryoscopically in cyclohexane) between that of a monomer and a dimer, even in the presence of added PBu_3. Since we can show by ^{31}P NMR that added PBu_3 exchanges rapidly, we believe the compound is a dimer with "ethylene" connecting two octahedral Zr(IV) centers (eq 5). Unfortunately, we could not confirm that the "ethylene" actually was aliphatic since its resonances in both the ^1H and ^{13}C spectra are obscured by the comparatively large PBu_3 resonances.

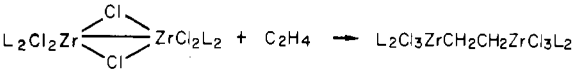
(5)

L = PR_3

$[ZrCl_3(PEt_3)_2]_2$ reacts with propylene to give dark yellow plates of toluene-soluble $[ZrCl_3(PEt_3)_2]_2(CH_2CHCH_3)$. The low-temperature ^{31}P NMR spectrum (−40 °C) show two types of phosphine ligands (not coupled), as expected for a dimer containing a "bridging propylene" (eq 6). At higher temperatures the two ^{31}P signals coalesce to a single broad peak. Fortunately, we could see the resonances for the bridging CH_2CHMe group at 14.9 (t, J_{CH} = 129 Hz), 8.09 (d, J_{CH} =

$$[ZrCl_3(PEt_3)_2]_2 + MeCH{=}CH_2 \xrightarrow{\text{toluene}} (PEt_3)_2Cl_3ZrCH_2CHMeZrCl_3(PEt_3)_2 \qquad (6)$$

---

(5) Pauling, L. "The Nature of the Chemical Bond", 3rd ed.; Cornell University Press: Ithaca, NY, 1960; p 260.

127 Hz), and 5.60 ppm (q, J_{CH} = 129 Hz) in the ^{13}C NMR spectrum. The fact that the CH coupling constants are strictly aliphatic confirms that propylene and ethylene "insert" into the Zr(III)–Zr(III) bond to give a dimer containing two C–Zr(IV) bonds.

Butadiene reacts with $[ZrCl_3(PEt_3)_2]_2$ rather differently. One equivalent reacts immediately to give a deep red solution whose 25 °C ^1H and ^{13}C NMR spectra suggest that butadiene is bound symmetrically. However, the reaction is reversible; $[ZrCl_3(PEt_3)_2]_2$ is the only species which crystallizes from these solutions, ultimately in high yield. Since PEt_3 is labile in $[ZrCl_3(PEt_3)_2]_2$, we believe butadiene displaces one or two phosphines to give a monoadduct, $[ZrCl_3(PEt_3)_x]_2(C_4H_6)$. If excess butadiene is added, the red solution turns orange after 1 h. Addition of pentane to a toluene solution yields yellow-orange $ZrCl_4(PEt_3)_2$, quantitatively. Pentane-soluble $ZrCl_2(C_8H_{12})(PEt_3)$ can be isolated from the filtrate. Finally, 1 equiv of free $PEt_3/ZrCl_2(C_8H_{12})(PEt_3)$ is observed by ^{31}P NMR. Therefore, the reaction of $[ZrCl_3(PEt_3)_2]_2$ with butadiene proceeds as shown in eq 7.

$$[ZrCl_3(PEt_3)_2]_2 + C_4H_6 \xrightarrow{\text{toluene}} Zr_2Cl_6(PEt_3)_{4-x}(C_4H_6) + xPEt_3 \xrightarrow{+C_4H_6} ZrCl_4(PEt_3)_2 + ZrCl_2(C_8H_{12})(PEt_3) + PEt_3 \quad (7)$$

The ^{13}C NMR spectrum of $ZrCl_2(C_8H_{12})(PEt_3)$ shows four major types of C_8H_{12} carbon atoms which are coupled to protons by 133–149 Hz and to phosphorus by up to 3 Hz. (The PEt_3 is *not* exchanging rapidly in this complex.) Four similar resonances due to a minor product are found close to the resonances of the major isomer. The ratio of isomers is ~9:1. A molecular weight measurement shows $ZrCl_2(C_8H_{12})(PEt_3)$ to be a monomer in benzene.

Two pieces of data suggest that $ZrCl_2(C_8H_{12})(PEt_3)$ contains allyl-like ligands. First, the IR spectrum shows a moderate strength peak at 1530 cm^{-1} characteristic of an allyl ligand.[6] (In $Zr(\eta^3\text{-}C_3H_5)_4$ it is found at 1520 cm^{-1}.[7]) Second, it reacts with HCl in C_6D_6 to give largely an organic product which by ^{13}C NMR is a symmetric, internal diene and which by GLC retention time contains eight carbons. Most likely it is *trans,trans*-2,6-octadiene. Therefore we believe $ZrCl_2(C_8H_{12})(PEt_3)$ is a bis η^3-allyl complex with a C_8 backbone formed from two butadiene molecules. Since each isomer has a mirror plane or a C_2 axis, they probably are closely related. Three reasonable possiblities are

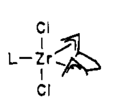

cisoid,syn,syn

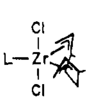

cisoid,anti,anti

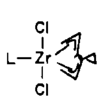

transoid,syn,syn

Discussion

$[ZrCl_3(PBu_3)_2]_2$ is the only structurally well-characterized adduct of $ZrCl_3$. Nitrogen donor adducts of ZrX_3 (X = Cl, Br, I) have been prepared, and some of them such as the pyridine[8,9] and lutidine[10] complexes have the stoichiometry $ZrCl_3L_2$. Fowles proposed[9] that such molecules are dimers with bridging halides since they have lower than expected magnetic moments for Zr(III). Unfortunately, however, they are relatively insoluble and not amenable to thorough study.

Tantalum[11] and tungsten[12] analogues of $[ZrCl_3(PBu_3)_2]_2$ are known, and the structure of $[TaCl_3(PMe_3)_2]_2$ has been determined.[11b] The structure of $[WCl_3(PMe_3)_2]_2$ has not been determined, but by ^{31}P NMR spectroscopy[12] it appears to be isostructural with $[WCl_3(py)_2]_2$.[13] In the Ta and W complexes the donor ligands occupy cis positions on one metal and trans positions on the other, in contrast to the "cis,cis" structure for $[ZrCl_3(PBu_3)_2]_2$ found here. The Ta_2Cl_2 and W_2Cl_2 cores are similar (see below) even though the Ta–Ta bond is formally a double bond and the W–W bond formally a single or triple bond. It is clear that the Zr_2Cl_2 core, however, contains only a relatively long, single metal–metal bond. Therefore the Cl–Zr–Cl angle is significantly smaller and the Zr–Cl–Zr angle considerably larger than the respective angles in the Ta and W complexes.

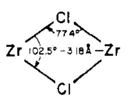

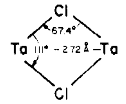

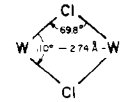

The Zr–Zr bond length in $[ZrCl_3(PBu_3)_2]_2$ (3.182 (1) Å) is close to that in zirconium metal (3.1789 Å in hexagonal β-Zr[14]) and slightly larger than that in β-$ZrCl_3$[15] (3.07 Å), a compound whose structure consists of chains of octahedra joined through opposite faces. (The low magnetic moment for β-$ZrCl_3$[16] also suggests a substantial Zr–Zr interaction.) Since the Zr–Cl (terminal) distance in $[ZrCl_3(PBu_3)_2]_2$ is 2.54 Å, we can estimate the covalent radius of Zr(III) as 1.55 Å (Cl^- = 0.99 Å[17]) and an appropriate Zr(III)–Zr(III) bond length as 3.10 Å. This is further evidence that the Zr–Zr bond in $[ZrCl_3(PBu_3)_2]_2$ is long and weak.

The "ethylene bridge" between two Zr(IV) centers has precedent. In 1966 Sinn[18] reacted $ZrCp_2Cl_2$ (Cp = η^5-C_5H_5) with $AlEt_3$ and isolated $Cp_2Zr(ClAlEt_3)(\mu\text{-}CH_2CH_2)(ClAlEt_3)ZrCp_2$ and $Cp_2Zr(Cl)(\mu\text{-}CH_2CH_2)(Cl)ZrCp_2$. He postulated an intermolecular abstraction of a β-hydrogen atom from one ZrEt group by another ZrEt group to give ethane and the $Zr(\mu\text{-}CH_2CH_2)Zr$ group. This was consistent with the results employing $Al(CD_2CH_3)_3$. The labeling study appears to rule out the possibility that $ZrCp_2Cl_2$ is first reduced to $[ZrCp_2Cl]_2$ and that $[ZrCp_2Cl]_2$ then reacts with ethylene (formed by disproportionation of ethyl radicals) in a manner analogous to that we observe here.

The coupling of butadiene ligands to give diallyl ligands has ample precedent in nickel chemistry.[19] It also has precedent in zirconium chemistry. Kablitz and Wilke[20] reported that $Zr(\eta^8\text{-}C_8H_8)(\eta^3\text{-}C_3H_5)_2$ reacts with excess butadiene to give a physically similar compound with the formula $Zr(\eta^8\text{-}C_8H_8)(C_8H_{12})$ which they propose contains a bis allyl C_8H_{12} ligand. This complex reacts with propanol to give (besides cyclooctatriene) *cis*- (mainly) and *trans*-1,6-octadiene and is a catalyst for dimerizing butadiene to *trans*-1,3,6-octatriene.

---

(6) Maslowsky, E. "Vibrational Spectra for Organometallic Compounds"; Wiley: New York, 1977; p 267.

(7) Ballard, D. G. H.; Jones, W. H.; Medinger, T. *J. Chem. Soc. B* **1968**, 1168–1175.

(8) Fowles, G. W. A.; Russ, B. J.; Wiley, G. R. *Chem. Commun.* **1967**, 646–647.

(9) Fowles, G. W. A.; Wiley, G. R. *J. Chem. Soc. A* **1968**, 1435–1438.

(10) Larsen, E. M.; Henzler, T. E. *Inorg. Chem.* **1974**, *13*, 581–587.

(11) (a) Fellmann, J. Ph.D. Thesis, MIT, 1980. (b) Sattelberger, A. P.; Wilson, R. B., Jr.; Huffman, J. C. *J. Am. Chem. Soc.* **1980**, *102*, 7111–7113.

(12) Sharp, P.; Schrock, R. R. *J. Am. Chem. Soc.* **1980**, *102*, 1430–1431.

(13) Jackson, R. B.; Streib, W. E. *Inorg. Chem.* **1971**, *10*, 1760–1763.

(14) Pearson, W. B. "A Handbook of Lattice Spacings and Structures of Metals and Alloys"; Pergamon: New York, 1967; Vol. 2, p 90.

(15) (a) Dahl, L. F.; Chiang, T.; Seabaugh, P. W.; Larsen, E. M. *Inorg. Chem.* **1964**, *3*, 1236–1242. (b) Watts, J. A. *Ibid.* **1966**, *5*, 281–283.

(16) Lewis, J.; Machin, D. J.; Newnham, I. E.; Nyholm, R. S. *J. Chem. Soc.* **1962**, 2036.

(17) Huheey, J. E. "Inorganic Chemistry", 2nd ed.; Harper and Row: New York, 1978; p 232.

(18) Sinn, H.; Kolk, E. *J. Organomet. Chem.* **1966**, *6*, 373–383.

(19) Jolly, P. W.; Wilke, G. "The Organic Chemistry of Nickel"; Academic Press: New York, 1974; Vol. I.

(20) Kablitz, H.-J.; Wilke, G. *J. Organomet. Chem.* **1973**, *51*, 241–271.

ZrCl$_2$(C$_8$H$_{12}$)(PEt$_3$) is not a catalyst for dimerizing butadiene. After several days at 60 °C in the presence of butadiene (~20 psi), some dark precipitate is formed, some ZrCl$_2$(C$_8$H$_{12}$)(PEt$_3$) can be recovered, and no C$_8$ organic products can be detected.

It is interesting to note that Wreford has reduced ZrCl$_4$(dmpe)$_2$ in the presence of butadiene to give [Zr(η^4-C$_4$H$_6$)$_2$(dmpe)]$_2$(dmpe) or Zr(η^4-C$_4$H$_6$)$_2$(dmpe).[21] The butadiene ligands have not coupled since protonolysis gives butenes. Almost certainly [ZrCl$_3$(dmpe)]$_2$ could be prepared in the absence of butadiene, although it would probably be only sparingly soluble. In the presence of butadiene either hypothetical ZrCl$_2$(C$_8$H$_{12}$)(dmpe) does not form (due possibly to the fact that dmpe is a chelating ligand) or, we feel less likely, reduction of ZrCl$_2$(C$_8$H$_{12}$)(dmpe) leads to cleavage of the C–C bond and formation of the zirconium(0)–bis(butadiene) complex.

Experimental Section

All experiments were performed under prepurified nitrogen in a Vacuum Atmospheres HE-43 drybox using solvents which had been rigorously dried under nitrogen by standard techniques.

Crystallographic Studies. Green, cube-shaped crystals of [ZrCl$_3$(PBu$_3$)$_2$]$_2$ were grown from toluene/pentane. The crystals are monoclinic, and the space group is $C2/c$ (C^6_{2h}, No. 15).[22]

An irregularly shaped crystal with minimum and maximum dimensions of 0.55 and 0.70 mm, respectively, was glued to the inside of a thin-walled glass capillary, and the capillary was sealed under nitrogen. This crystal was then accurately centered optically on a computer-controlled four-circle Nicolet autodiffractometer, and a total of 15 high-angle ($2\theta_{\mathrm{Mo}\,K\bar{\alpha}} > 30°$) reflections, chosen to give a good sampling of reciprocal space and diffractometer settings, were used to align the crystal and calculate angular settings for each reflection. A least-squares refinement of the diffraction geometry for these 15 reflections recorded at ambient temperature (20 ± 1 °C) with graphite-monochromated Mo K$\bar{\alpha}$ radiation (λ = 0.710 73 Å) gave the lattice constants a = 26.570 (6) Å, b = 15.287 (3) Å, c = 16.452 (3) Å, and β = 97.18 (2)°. A unit cell content of four dimers gave a calculated density of 1.21 g/cm^{-3}. The linear absorption coefficient was 6.7 cm^{-1}.[23]

Intensity measurements utilized graphite-monochromated Mo K$\bar{\alpha}$ radiation and the ω scanning technique with a 4° takeoff angle and a normal-focus X-ray tube. For those reflections having $2\theta < 43°$, a scanning rate of 6.0°/min was employed for the scan between ω settings 0.45° above and below the calculated K$\bar{\alpha}$ doublet value of each reflection. A scanning rate of 4.0° min^{-1} was used for reflections having $43° < 2\theta < 55°$. Each 0.9° scan was divided into 19 equal time intervals, and those 13 contiguous intervals which had the highest single accumulated count at their midpoint were used to calculate the net intensity from scanning. A careful and systematic preliminary study of peak widths (half-height to half-height) indicated a nearly constant peak width of 0.35° in ω for all orientations of the crystal. Background counts, each lasting one-fourth the total time for the net scan, were measured at ω settings 0.90° above and below the calculated value for each reflection.

A total of 7637 independent reflections having $2\theta < 55.0°$ (the equivalent of 1.0 limiting Cu K$\bar{\alpha}$ spheres) were measured in concentric shells of increasing 2θ containing approximately 3800 reflections each. The six standard reflections, measured every 300 reflections as a monitor for possible misalignment and/or deterioration of the crystal, gave no indication of either. The intensities were empirically corrected for absorption using psi scans for seven representative reflections before they were reduced to a set of relative squared amplitudes, $|F_o|^2$, by means of standard Lorentz and polarization corrections.

After the atomic coordinates to the zirconium atoms were derived from a three-dimensional Patterson synthesis, the remaining nonhydrogen atoms of the totally general-position asymmetric unit were located from a series of least-squares refinement cycles followed by difference Fourier syntheses. Unit-weighted full-matrix least-squares refinement of the fractional atomic coordinates and isotropic thermal parameters of the 30 crystallographically independent nonhydrogen atoms resulted in a conventional unweighted residual of 0.084 ($R_1 = \sum||F_o| - |F_c||/\sum|F_o|$) and a conventional weighted residual of 0.084 ($R_2 = [\sum w(|F_o| - |F_c|)^2/\sum w|F_o|^2]^{1/2}$) for 3057 independent reflections having $2\theta < 43°$ and $I > 3\sigma(I)$. Utilization of anisotropic thermal parameters for all nonhydrogen atoms in further cycles of empirically weighted least-squares refinement using the more complete data set gave R_1 = 0.053 and R_2 = 0.062 for 4720 reflections having $2\theta_{\mathrm{Mo}\,K\alpha} < 55°$ and $I > 3\sigma(I)$.

Preparation of [ZrCl$_3$L$_2$]$_2$. ZrCl$_4$ (6.0 g, 25.8 mmol), PEt$_3$ (6.08 g, 51.5 mmol), and 0.41% NaHg (145 g, 25.8 mmol) were stirred together in 100 mL of toluene for 3 h. the reaction mixture was filtered through Celite, and the solids were extracted with 1 L of toluene. The toluene was removed from the filtrate in vacuo, and crops of forest green plates were collected periodically; the total yield was 7.6 g (68%). [ZrCl$_3$(PPr$_3$)$_2$]$_2$ and [ZrCl$_3$(PBu$_3$)$_2$]$_2$ were prepared analogously. They are progressively more soluble in toluene.

Anal. Calcd for [ZrCl$_3$(PEt$_3$)$_2$]$_2$ (ZrC$_{12}$H$_{30}$P$_2$Cl$_3$): C, 33.22; H, 6.97. Found: C, 33.35; H, 6.87. ^{31}P{^{1}H} NMR of [ZrCl$_3$(PEt$_3$)$_2$]$_2$ (C$_6$D$_6$): δ –3.82 (br s). ^{31}P{^{1}H} NMR of [ZrCl$_3$(PBu$_3$)$_2$]$_2$ (toluene-d_8, –30 °C): δ –8.73 (s).

Reaction of [ZrCl$_3$(PEt$_3$)$_2$]$_2$ with TlCp. [ZrCl$_3$(PEt$_3$)$_2$]$_2$ (0.87 g, 1.0 mmol) and TlCp (0.54 g, 2.0 mmol) were stirred together in 5 mL of toluene for 1.5 h. Malleable, silvery nuggests of thallium metal were filtered off the reaction mixture, and the toluene was removed from the filtrate in vacuo, yielding 0.84 g (80%) of pale yellow ZrCpCl$_3$(PEt$_3$)$_2$. A small amount of ZrCp$_2$Cl$_2$ was present as an impurity. ZrCpCl$_3$(PEt$_3$)$_2$ was prepared independently from ZrCpCl$_3$.[24]

^{1}H NMR of ZrCpCl$_3$(PEt$_3$)$_2$ (C$_6$D$_6$): δ 6.28 (s, 5, Cp), 1.30, 0.85 (br m, 30, PEt$_3$).

Preparation of [ZrCl$_3$(PBu$_3$)$_2$]$_2$(CH$_2$CH$_2$). A 10-mL pressure bottle containing a solution of [ZrCl$_3$(PBu$_3$)$_2$]$_2$ (0.5 g, 0.42 mmol) in 2 mL of pentane was pressurized to 30 psi with ethylene. The green solution turned orange immediately. The solution was filtered, and the volume of the filtrate was reduced in vacuo. After the solution was stored overnight at –30 °C, 0.47 g (95%) of orange prisms were collected by filtration.

Anal. Calcd for ZrC$_{25}$H$_{36}$P$_2$Cl$_3$: C, 48.73; H, 9.16. Found: C, 48.49; H, 9.27. ^{31}P{^{1}H} NMR (toluene-d_8, –60 °C): –7.49 (s, PBu$_3$).

Preparation of [ZrCl$_3$(PEt$_3$)$_2$]$_2$(CH$_2$CHCH$_3$). A 10-mL pressure bottle containing a solution of [ZrCl$_3$(PEt$_3$)$_2$]$_2$ (0.5 g, 0.58 mmol) in 3 mL of toluene was pressurized with propylene to 40 psi, and the reaction mixture was stirred for 10 h. Activated charcoal was added to the dark yellow solution, and the solution was stirred for 30 min. The mixture was filtered, and the volume was reduced in vacuo. A small volume of pentane was added, and the solution was stored at –30 °C overnight. A total of 0.42 g (90%) of dark yellow plates were collected by filtration.

^{13}C NMR (C$_6$D$_6$, gated ^{1}H decoupled): δ 15.9 (t, J_{CH} = 130 Hz, P*C*H$_2$CH$_3$), 14.9 (t, J_{CH} = 129 Hz, H$_2$*C*CHCH$_3$), 8.09 (d, J_{CH} = 127 Hz, H$_2$C*C*HCH$_3$), 7.52 (q, J_{CH} = 128 Hz, PCH$_2$*C*H$_3$), 5.60 (q, J_{CH} = 129 Hz, CH$_2$CH*C*H$_3$). ^{31}P{^{1}H} NMR (toluene-d_8, –40 °C): δ –1.93 (s), –3.94 (s).

Preparation of ZrCl$_2$(C$_8$H$_{12}$)(PEt$_3$). A total of 2 mL of butadiene was condensed into a 10-mL pressure bottle containing a solution of [ZrCl$_3$(PEt$_3$)$_2$]$_2$ (0.8 g, 0.92 mmol) in 2 mL of toluene. The color of the reaction mixture changed from green to red immediately and then to orange after 1 h. The reaction mixture was filtered, and the volume was reduced in vacuo to ~0.5 mL. Pentane (5 mL) was added, and the solution was stored at –30 °C overnight. A total of 0.42 g (98%) of yellow-orange needles of ZrCl$_4$(PEt$_3$)$_2$ was collected by filtration. The solvent was removed from the filtrate in vacuo, and the oily residue was extracted into a minimal amount of pentane. The solution was stored at –30 °C overnight to give 0.35 g (95%) of orange prisms of ZrCl$_2$(C$_8$H$_{12}$)(PEt$_3$).

Anal. Calcd for ZrCl$_4$(PEt$_3$)$_2$ (ZrC$_{12}$H$_{30}$P$_2$Cl$_4$): C, 30.71; H, 6.44. Found: C, 31.10; H, 6.64. Calcd for ZrCl$_2$(C$_8$H$_{12}$)(PEt$_3$) (ZrC$_{14}$H$_{27}$PCl$_2$): C, 43.28; H, 7.01. Found: C, 42.70; H, 7.04. ^{13}C NMR of ZrCl$_2$(C$_8$H$_{12}$)(PEt$_3$) (C$_6$D$_6$, gated ^{1}H decoupled): δ 141.9

---

(21) (a) Datta, S.; Wreford, S. S.; Beatty, R. P.; McNeese, T. J. *J. Am. Chem. Soc.* **1979**, *101*, 1053–1054. (b) Beatty, R. P.; Datta, S.; Wreford, S. S. *Inorg. Chem.* **1979**, *18*, 3139–3145.

(22) "International Tables for X-Ray Crystallography"; Kynoch Press: Birmingham, England, 1969; Vol. I.

(23) "International Tables for X-Ray Crystallography"; Kynoch Press: Birmingham, England, 1974; Vol. IV, pp 55–56.

(24) Reid, A. F.; Wailes, P. C. *J. Organomet. Chem.* **1964**, *2*, 329.

(d, J_{CH} = 149 Hz, J_{CP} = 2.9 Hz, $\mathrm{H_2C\overset{\dots}{-}\mathit{C}H\overset{\dots}{-}CHCH_2}$), 117.6 (d, J_{CH} = 141 Hz, $\mathrm{H_2C\overset{\dots}{-}CH\overset{\dots}{-}\mathit{C}HCH_2}$), 66.4 (dd, AB, J_{CH} = 146.5 and 145.5 Hz, J_{CP} = 3.9 Hz, $\mathrm{H_2\mathit{C}\overset{\dots}{-}CH\overset{\dots}{-}CHCH_2}$), 41.0 (t, J_{CH} = 133 Hz, $\mathrm{H_2C\overset{\dots}{-}CH\overset{\dots}{-}CH\mathit{C}H_2}$), 17.3 (dt, J_{CH} = 135 Hz, J_{CP} = 13.7 Hz, $\mathrm{P\mathit{C}H_2CH_3}$), 7.73 (dq, J_{CH} = 129 Hz, J_{CP} = 1.9 Hz, $\mathrm{PCH_2\mathit{C}H_3}$). The minor isomer has analogous C_8H_{14} peaks at 144.5, 109.4, 68.7, and 38.8 ppm. $^{31}P\{^1H\}$ NMR of $ZrCl_2(C_8H_{12})(PEt_3)$ (C_6D_6): δ -2.27 (s). IR (Nujol): 1530 cm^{-1} (br, m) ($\nu_{C\overset{\dots}{-}C\overset{\dots}{-}C}$).

Acknowledgment. We thank the National Science Foundation for generously supporting this research (Grant CHE 79 05307).

Registry No. $[ZrCl_3(PBu_3)_2]_2$, 77061-29-1; $[ZrCl_3(PPr_3)_2]_2$, 77061-30-4; $[ZrCl_3(PEt_3)_2]_2$, 77061-31-5; $[ZrCl_3(PBu_3)_2]_2(CH_2CH_2)$, 77061-32-6; $[ZrCl_3(PEt_3)_2]_2(CH_2CHCH_3)$, 77061-33-7; $ZrCl_2(C_8H_{12})(PEt_3)$, 77061-34-8; $ZrCl_4(PEt_3)_2$, 77061-35-9; $ZrCpCl_3(PEt_3)_2$, 77061-36-0; C_2H_4, 74-85-1; $MeCH{=}CH_2$, 115-07-1; C_4H_6, 106-99-0; TlCp, 34822-90-7.

Supplementary Material Available: Listings of anisotropic thermal parameters for nonhydrogen atoms of $[ZrCl_3(PBu_3)_2]_2$ (Table II) and observed and calculated structure factors from the final cycle of least-squares refinement (22 pages). Ordering information is given on any current masthead page.

Contribution from 3M Central Research Laboratories, St. Paul, Minnesota 55101,
and the Department of Chemistry, University of Minnesota, Minneapolis, Minnesota 55455

1:1 Lewis Base Adducts of Palladium Bis(hexafluoroacetylacetonate) and the Structure of $Pd(F_6acac\text{-}\mathit{C})(F_6acac\text{-}\mathit{O,O})\cdot(CH_3)_2NH$

A. R. SIEDLE* and L. H. PIGNOLET

Received October 16, 1980

A series of 1:1 Lewis base adducts of palladium bis(hexafluoroacetylacetonate) of the type $Pd(F_6acac)_2\cdot L$ were prepared where L = 2,6-dimethylpyridine (**1**), 2,4,6-trimethylpyridine (**2**), phenoxathiin (**3**), phenazine (**4**), and dimethylamine (**5**). These compounds contain four-coordinate palladium with one carbon-bonded hexafluoroacetylacetonate (F_6acac-*C*) and one bidentate oxygen-bonded (F_6acac-*O,O*) ligand. This bonding pattern can be recognized by the 1:1:2 pattern of singlets in the ^{19}F NMR and by a strong infrared band at 1750-1730 cm^{-1} due to the $(CF_3CO)_2CH$ fragment. The structure of $Pd(F_6acac)_2\cdot(CH_3)_2NH$ (**5**) was determined by single-crystal X-ray diffraction. Crystal data: space group *Pbca* (No. 61), *a* = 15.448 (5) Å, *b* = 15.567 (5) Å, *c* = 16.178 (3) Å, *V* = 3891 $Å^3$, *Z* = 8. The palladium coordination is square planar and the nearly symmetrical oxygen-bonded F_6acac-*O,O* ligand has a *d*(Pd-O) trans to nitrogen of 2.002 (4) Å and *d*(Pd-O) trans to carbon of 2.059 (5) Å. The palladium-nitrogen separation is 2.028 Å. The $(CF_3CO)_2CH$ moiety is approximately planar, and the dihedral angle between its plane and the palladium coordination plane is 88.4°. The Pd-F_6acac-*C* distance is 2.101 (7) Å.

We have previously reported that palladium bis(hexafluoroacetylacetonate), $Pd(F_6acac)_2$, has a novel and extensive acid-base chemistry. The fluorinated metalloorganic compound forms four classes of adducts with Lewis bases, L, of the type $Pd(F_6acac)_2\cdot nL$, where *n* = 1-4.[1] As part of a systematic investigation of these materials, the 1:1 adducts of $Pd(F_6acac)_2$ have been studied in detail. This paper reports their synthesis and properties and the structure of an exemplary member of the *n* = 1 class, $Pd(F_6acac)_2\cdot(CH_3)_2NH$.

Synthesis and Properties

1:1 adducts of $Pd(F_6acac)_2$ may be prepared by direct reaction with a Lewis base in nonpolar organic solvents (cf. Experimental Section). The stability of $Pd(F_6acac)_2\cdot L_n$ with *n* = 1 relative to the *n* = 2 or 4 class appears to be determined in large part by the steric properties of the base. Thus, while pyridine reacted with $Pd(F_6acac)_2$ to yield 4:1 $Pd(F_6acac)_2\cdot 4C_5H_4N$, the more hindered 2,6-dimethylpyridine formed only $Pd(F_6acac)_2\cdot 2,6\text{-}Me_2C_5H_3N$ (**1**). With other ligands which are sterically less demanding, such as dimethylamine, 1:1, 2:1, or 4:1 adducts were obtained by adjusting the reaction conditions.

The spectroscopic properties of **1** have been studied in detail since this was one of the first $Pd(F_6acac)_2$ complexes in which the structure could be reasonably inferred from NMR and infrared data and because complexes of this type have been identified as intermediates in ortho-metalation reactions of $Pd(F_6acac)_2$.[1] **1** and the other compounds reported of the $Pd(F_6acac)_2\cdot L_n$ (*n* = 1) class have one carbon-bonded F_6acac ligand (F_6acac-*C*) and one bidentate F_6acac group bonded through the oxygen atoms (F_6acac-*O,O*). The F_6acac-*C* or, alternatively, bis(trifluoroacetyl)methyl function contains two uncoordinated CF_3CO groups which are distinguished by a strong infrared absorption at 1750 cm^{-1} and by a singlet of relative area 6 at 77.50 ppm in the ^{19}F NMR spectrum. In the ^{13}C spectrum, the methine carbon doublet is at rather high field (δ 29.5) with J_{C-H} = 144 Hz, which is reasonable for a sp^3 carbon bonded to two electronegative groups. Double irradiation experiments showed that the proton with δ 4.99 is coupled to this carbon atom, and it is assigned to the $(CF_3CO)_2CH$ group.

The C=O vibrations in the bidentate F_6acac-*O,O* function are, by analogy with other metal acetylacetonates,[2] probably not pure modes, and so the 1705- and 1640-cm^{-1} bands provide, at the present level of experience, little definitive structural information. The two CF_3 groups in this ligand are chemically nonequivalent since one bears a transoid relationship to carbon in F_6acac-*C* and the other is opposite the pyridine nitrogen, and so two closely spaced singlets at 75.07 and 75.12 ppm in the ^{19}F NMR spectrum are seen. Thus, a 1:1:2 pattern of singlets appears to be characteristic of most carbon-bonded $Pd(F_6acac)_2\cdot L$ compounds. The F_6acac-*O,O* methine carbon has δ 92.2 and J_{C-H} = 169 Hz. The methine proton at δ 6.30 is considerably less shielded than its counterpart in the F_6acac-*C* moiety.

The methyl groups at the 2,6 positions in the pyridine ring are also deshielded. The ^1H and ^{13}C shifts are 3.26 and 26.7 ppm (J_{C-H} = 128 Hz), respectively, compared with 2.52 and 19.0 ppm in the free base. This effect is due to the magnetic anisotropy associated with the tetragonal d^8 system which occurs when the pyridine ring is twisted so that it is nearly perpendicular to the PdO_2CN plane, a geometry observed in $(2,4,6\text{-}Me_3py)PtCl_2(C_2H_4)$.[3] The absence of large pertur-

---

[1] A. R. Siedle and L. H. Pignolet, submitted for publication.

[2] K. Nakamoto, P. J. McCarthy, A. Ruby, and A. E. Martell, *J. Am. Chem. Soc.*, **83**, 1006, 1272 (1961).

0020-1669/81/1320-1849$01.25/0